A multi-scale computational strategy for structured thin sheets

E.W.C. Coenen[1,2], V.G. Kouznetsova[1,2], M.G.D. Geers[1]

[1]*Faculty of Mechanical Engineering, Eindhoven University of Technology - PO Box 513, 5600 MB Eindhoven, The Netherlands*
URL: www.mate.tue.nl e-mail: E.W.C.Coenen@tue.nl; V.G.Kouznetsova@tue.nl; M.G.D.Geers@tue.nl
[2]*Netherlands Institute for Metals Research - PO Box 5008, 2600 GA Delft, The Netherlands*
URL: www.NIMR.nl

ABSTRACT: Engineering trends show an increasing use of multi-layered and structured thin sheets in innovative applications where the layer thickness approaches the microstructural scale. This paper presents a strategy to homogenize the actual three-dimensional heterogeneous sheet towards a shell continuum. Consistent scale transition relations are derived, providing the ability to solve the (generalized) stress-strain fields on both the microstructural and the engineering scale are obtained in a direct and coupled manner.

Key words: FE^2, coarse graining, structured thin sheets, computational homogenization, structural analysis, multi-scale mechanics

1 INTRODUCTION

Engineering trends show an increasing use of multi-layered and structured thin sheets in innovative applications, e.g. composite and sandwich panels, functional materials and ultra-thin sheets, where layer thickness may approach the microstructural scale. The analysis of forming process, application performance and life prediction of thin sheets is typically based on shell elements. In the case of sheets composed of different materials with complex (through-layer) geometries or interactions between different layers, the use of classical layer-wise composite shell theory is not possible. For these applications, a two-scale computational homogenization technique for thin structured sheets is proposed within this work.

Computational homogenization is a powerful multi-scale technique that fully exploits the coupling between mechanics at different length scales. It relies on the nested solution algorithm of two coupled boundary value problems (BVP), and directly provides stress and strain field in equilibrium at both scales, (FE^2). Such a multi-scale approach (i) does not require any constitutive assumptions on the macrolevel, (ii) enables the incorporation of large deformations at both scales, (iii) is suitable for arbitrary material behavior and complex microstructural geometries, and (iv) allows the use of any modeling technique on the microlevel, e.g. the finite element method.

The first scheme introduced was a first-order computational homogenization framework for solids, where only the first gradient of the macroscopic displacement field was included in the scale transition. This resulted in a classical continuum description at both scales, yet lacking the possibility to capture microstructural size effects. This was partially solved, by the introduction of a second-order computational homogenization scheme based on a macro-micro coupling of both the first and the second gradient of the displacement field [3]. The macroscopic problem described by a second-order equilibrium equation, is able to capture more complex deformation modes (e.g. bending) due the characteristic length passed through the scale transition.

In shell theories, physically 3D sheets are typically represented by 2D surfaces in space. The equilibrium equation includes both generalized stress and couple-stress (moments) results and is intrinsically a second-order type problem. The computational homogenization of structured thin sheets can be considered as a special case of the second-order homogenization of continua [2], which is presented in this paper.

Throughout the paper a co-rotational formulation of the orthogonal coordinate system is used. The first $\vec{e}_1$ and second $\vec{e}_2$ principle directions are tangent to the shell's midplane, consequently the third direction $\vec{e}_3$ is normal. Bold characters indicate tensor quantities and an additive decomposition of a vector $\vec{a}$ into an in-plane $\hat{\vec{a}}$ and transverse part $\tilde{\vec{a}}$ is used.

2 SHELL MECHANICS

Most shell formulations involves a number of assumptions on both the kinematics and statics of the underlying mechanical description. Here, the Kirchhoff-Love (KL) and the kinematically more rich Mindlin-Reissner (MR) theories, which are respectively known as thin and thick shell theories, are considered [1].

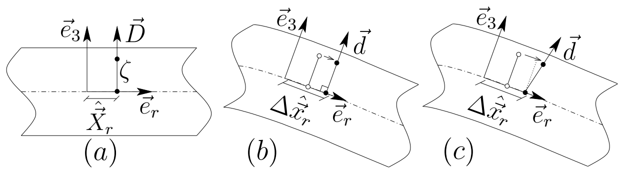

Figure 1: Reference configuration of a shell (a) and the deformed configuration of a KL (b) and MR (c) type shell.

The relative position of an arbitrary material point within the vicinity of a point (located at the origin of the local co-rotational coordinate system) on the midplane of an initially flat shell, in respectively the reference and the current configuration, is given by

$$\vec{X} = \vec{X}_r + \zeta\vec{D} \quad \text{and} \quad \Delta\vec{x} = \Delta\vec{x}_r + \zeta\vec{d} + \Delta\vec{w}. \tag{1}$$

Here, ζ is the out-of-plane coordinate measured along the directors $\vec{D} = \vec{e}_3$ (reference) and $\vec{d}$ (current), see figure 1. Upon deformation, a material line element along the initial director $\vec{D}$ is assumed to remain straight and inextensible. In KL shells, $\vec{d}$ is assumed to remain perpendicular to the midplane. In MR shells this constraint is relieved by allowing transverse shear. A micro-fluctuation field $\vec{w}$ is introduced to reflect the fine-scale contribution on top of the macro-scale kinematics. The in-plane displacements hold the key for elaborating the macro-micro scale transition and are expressed in generalized strains, which only have in-plane components, i.e.

$$\Delta\hat{\vec{u}} = (\boldsymbol{\mathcal{E}}_{\mathrm{M}} + \zeta\boldsymbol{\mathcal{K}}_{\mathrm{M}}) \cdot \hat{\vec{X}} + \zeta\hat{\vec{\gamma}}_{\mathrm{M}} + \Delta\hat{\vec{w}}. \tag{2}$$

[1]Definition in standard shell formulation

The terms containing the curvature tensor $\boldsymbol{\mathcal{K}}_{\mathrm{M}}$ and the transverse shear vector $\hat{\vec{\gamma}}_{\mathrm{M}}$ (not for KL shells) describe the in-plane displacement by the rigid rotation of the director. The term with the membrane strain tensor $\boldsymbol{\mathcal{E}}_{\mathrm{M}}$ reflects the contribution of the straining of the midplane. An alternative interpretation is to consider $\hat{\hat{\mathbf{F}}}_{\mathrm{M}} = (\boldsymbol{\mathcal{E}}_{\mathrm{M}} + \zeta\boldsymbol{\mathcal{K}}_{\mathrm{M}})$ as the in-plane gradient deformation tensor of each lamina, a parallel plane to the midplane at distance ζ.

The generalized forces (stress results) are defined as integrals over the shell thickness H, based on the first Piola-Kirchhoff stress tensor $\mathbf{P}$. The membrane force $\mathbf{N}_{\mathrm{M}}$, bending/twisting moments $\mathbf{M}_{\mathrm{M}}$, and the shear forces $\hat{\vec{Q}}_{\mathrm{M}}$, are respectively defined as [1]

$$\begin{aligned} \mathbf{N}_{\mathrm{M}} &= \int_H \hat{\hat{\mathbf{P}}}\mathrm{d}\zeta, \qquad \mathbf{M}_{\mathrm{M}} = \int_H \zeta\hat{\hat{\mathbf{P}}}\mathrm{d}\zeta, \\ \hat{\vec{Q}}_{\mathrm{M}} &= \vec{e}_3 \cdot \int_H \hat{\tilde{\mathbf{P}}}\mathrm{d}\zeta. \end{aligned} \tag{3}$$

3 COMPUTATIONAL HOMOGENIZATION

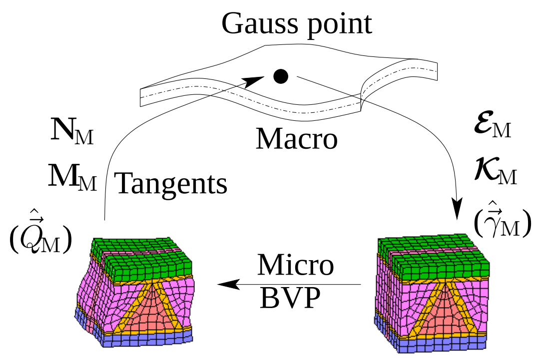

Figure 2: Schematic representation of the computational homogenization of structure thin sheets.

The constitutive response relating the defined generalized strain and force measures is directly extracted from the response of the underlying microstructure by computational homogenization, see figure 2.

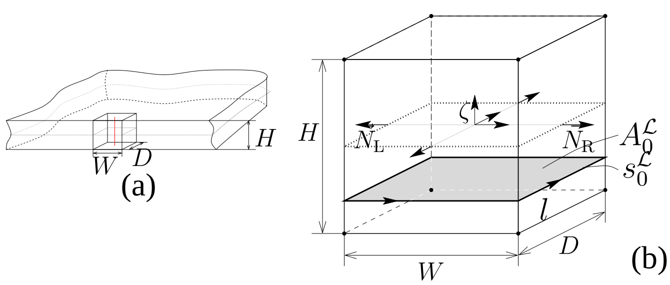

Figure 3: (a) The RVE depicted in a shell (b) and the through-thickness representative volume element (RVE).

A through-thickness RVE with finite in-plane dimensions, spanning a representative volume of the microstructure, is used. The RVE spans the full thickness of the shell H, and therefor implies a homogenization with respect to the midplane and a direct thickness-integration. The RVE is geometrically initially cuboidal with dimensions $W{\times}D{\times}H$, see figure 3 (left).

Kinematical scale transitions are established by controlling the micro-fluctuation $\hat{\vec{w}}$ introduced in equation 2. The first scale transition relation requires that the in-plane macroscopic deformation gradient tensor $\hat{\hat{\mathbf{F}}}_{\mathrm{M}}(\zeta)$ to be equal to the surface average of $\hat{\hat{\mathbf{F}}}_{\mathrm{m}}$ of each lamina. Using similar arguments as used in the elaboration of the second-order RVE [3], a generalized periodic boundary condition is used, which is based on the in-plane part of the field $\vec{w}$

$$\hat{\vec{w}}_L(l,\zeta) = \hat{\vec{w}}_R(l,\zeta) \qquad \forall \zeta \in [-H/2, H/2] \tag{4}$$

applying the local coordinate l on opposite faces L and R (left,right). Similar constraints are imposed to the back and front face of the RVE. The RVE's top and bottom faces are not constrained, implying (traction) free boundaries. Additional kinematical constraints (not derived here) in the third direction are imposed to keep the RVE on average tangent to the $\{\vec{e}_1, \vec{e}_2\}$-plane.

The boundary conditions related to transverse shear are more delicate, due to its related well-known kinematical inconsistency. The absence of global shear tractions in the micro-scale problem (plane strain condition) inhibits the directors form remaining straight (as assumed at the macro scale). Therefore, only a weak constraint is enforced on each of the lateral faces, requiring that the average micro-scale shear of the face is equal to the macroscopic value of the transverse shear, i.e. for the left face

$$\int_{\Gamma_{0L}} \zeta \hat{\vec{w}} \mathrm{d}\Gamma_0 = \hat{\vec{0}}. \tag{5}$$

All kinematical constraints can be written as tying relations, which are linear relations degrees of freedom, following a similar approach as the one used for second-order computational homogenization, [3].

Upon solution of the classical microstructural BVP, the generalized forces can be calculated according to their definitions extracted from the Hill-Mandel condition, showing a clear analogy with the standard definition in equation 3.

$$\mathbf{N}_{\mathrm{M}} = \frac{1}{WD}\int_{V_0} \hat{\hat{\mathbf{P}}}_{\mathrm{m}} \mathrm{d}V_0, \qquad \mathbf{M}_{\mathrm{M}} = \frac{1}{WD}\int_{V_0} \zeta \hat{\hat{\mathbf{P}}}_{\mathrm{m}} \mathrm{d}V_0,$$
$$\hat{\vec{Q}}_{\mathrm{M}} = \vec{e}_3 \cdot \frac{1}{WD}\int_{V_0} \tilde{\hat{\mathbf{P}}}_{\mathrm{m}} \mathrm{d}V_0 \tag{6}$$

In the descretized solution, the generalized forces can be directly calculated from the reaction forces on the prescribed control nodes. The macroscopic constitutive tangents can be extraction by condensation of the micro-stiffness matrix.

4 NUMERICAL EXAMPLE

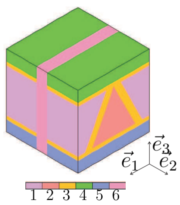

Mat.	E (GPa)	ν	σ_y (GPa)	h (GPa)
1,2	2.0	0.42	-	-
3	210	0.3	0.51	0.2
4,5	30	0.4	0.6	5
6	10	0.15	-	-

Figure 4: Substructured through-thickness 3D RVE.

To illustrate the computational homogenization of shells, a periodic microstructure composed of 3D RVEs with a complex through-thickness substructure is considered, see figure 4. The initial RVE is cubic with dimensions $1 \times 1 \times 1\mathrm{mm}^3$ and is discretized with 8-node 3D brick elements. Three typical macroscopic deformation modes, i.e. bending, twisting and shearing are considered, as shown in figure 5. The deformed RVEs show a pronounced non-uniform character in their displacement and stress field. The relevant generalized forces obtained, also show a clearly non-linear evolution. All these effects cannot be trivially captured in a closed-form macroscopic constitutive equation.

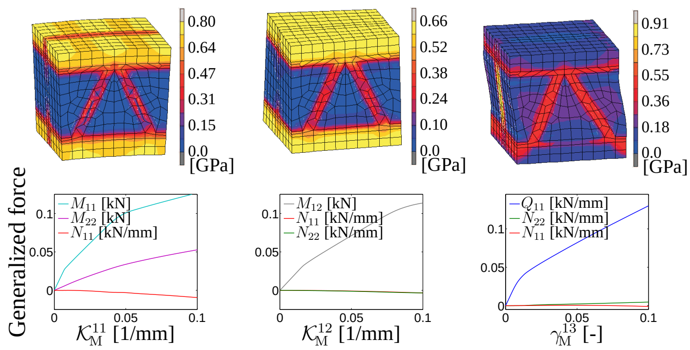

Figure 5: RVE deformations and distribution of the equivalent von Mises stress (top row) and macroscopic homogenized response for different RVE deformations modes (bottom row).

A fully coupled multi-scale example is next considered, i.e. a wide shell with the underlying microstructure shown in figure 4. It is clamped on its two ends and a vertical displacement w is described in its center, see figure 6. Only half the shell is modeled because of symmetry. The figure gives an overview of the two-scale solution of the problem with the deformed macroscopic shell and the global force-displacement curve, as well as the deformed microstructures with their local stress fields. The solution is compared with a full-scale reference solution.

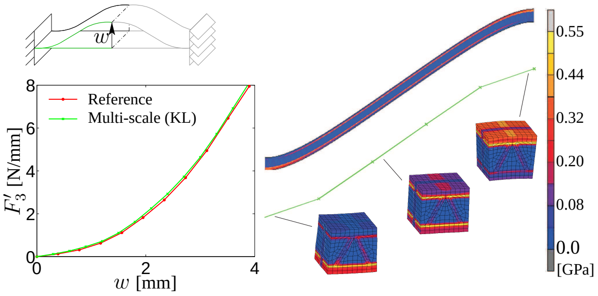

Figure 6: The global response and deformed profiles with eq. v.M. stress contour plots obtained with the KL multi-scale analysis of a shell and a reference continuum analysis.

The same heterogeneous shell is now considered, but with square dimensions and a thickness of 0.2mm. The RVE depicted in figure 4 is therefore scaled so that it is a cuboid with dimensions $0.3{\times}0.3{\times}0.2$ mm^3. The sheet is clamped at one edge and twisted by two opposite forces at the other edges. This twisting loading of the shell illustrates the capability of the computational homogenization framework to perform a fully 3D mechanical analysis, see figure 7. This analysis was performed with $5{\times}5$ 4-node KL-shell elements. A full-scale analysis would incorporate 300×300 RVEs stacked side by side, which is computationally very expensive.

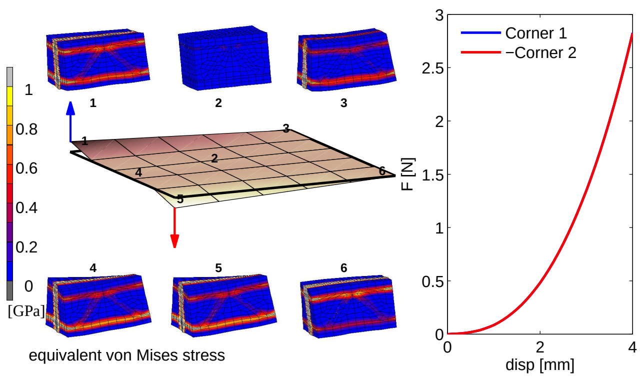

Figure 7: Multi-scale analysis (KL) of a heterogeneous sheet subjected to a twist load.

5 CONCLUSIONS

In this work, an overview was given of the main principles needed to construct a computational homogenization scheme that links up macroscopic shells to 3D through-thickness microstructural RVEs. Due to some macro-micro inconsistencies, constraints inherited from kinematical assumptions made in shell theory, need to be handled properly. The derivation of the generalized forces follows directly from the condition that the variation of work performed by the microstructure should equal the variation of work performed by the macrolevel, both expressed per unit area of the midplane.

Here, the macroscopic heterogeneous sheet is modeled by a shell-type boundary value problem derived from the classical shell theories, i.e. Kirchhoff-Love and Mindlin-Reissner. Evidently, the choice of the underlying shell theory has an influence on the scale transition derived, however the application to other shell formulations (e.g. solid like shell) can be readily obtained in a similar manner.

The computational effort of a fully coupled multi-scale analysis is significant, but this drawback is largely overcome through the parallelization of the multi-scale algorithm. A powerful tool for the analysis of structured thin sheets results, which can handle very complex, periodic microstructure. The multi-scale technique can be directly applied as a design tool for the development of microstructures such that the functionality and the resulting macroscopic behaviour exhibit the required characteristics.

REFERENCES

[1] T. Belytschko, W.K. Liu, and B. Moran. *Nonlinear Finite Elements for Continua and Structures*. O J. Wiley & Sons, New York, 2000.

[2] M.G.D. Geers, E.W.C. Coenen, and V.G. Kouznetsova. Multi-scale computational homogenization of structured thin sheets. *Model. Simul. Mater. Sci. Engng.*, 15:S393–S404, 2007.

[3] V.G. Kouznetsova, M.G.D. Geers, and W.A.M. Brekelmans. Multi-scale second-order computational homogenization of multi-phase materials: a nested finite element solution strategy. *Comput. Methods. Appl. Mech. Engrg.*, 193(48-51):5525–5550, 2004.